Infrared Spectroscopic Study of Stratum Corneum Model Membranes Prepared from Human Ceramides, Cholesterol, and Fatty Acids

G. S. Gooris and J. A. Bouwstra
Leiden/Amsterdam Center for Drug Research, Department of Drug Delivery Technology, Leiden University, 2300 RA Leiden, The Netherlands

ABSTRACT The outermost layer of the skin, the stratum corneum, consists of corneocytes surrounded by lipid domains. The main lipid classes in stratum corneum are cholesterol, ceramides (CER), and free fatty acids forming two crystalline lamellar phases. However, only limited information is available on whether the various lipid classes participate in the same crystalline lattices or if separate domains are formed within the lipid lamellae. In this article infrared spectroscopic studies are reported of hydrated mixtures prepared from cholesterol, human CER, and free fatty acids. Evaluation of the methylene stretching vibrations revealed a conformational disordering starting at ~60°C for all mixtures. Examination of the rotational ordering (scissoring and rocking vibrations) of mixtures prepared from equimolar cholesterol and CER with a variation in the level of free fatty acids showed that at lower free fatty acid content orthorhombic and hexagonal domains coexist in the lipid lamellae. Increasing the fatty acid level to an equimolar cholesterol/CER/fatty acid mixture reveals the dominant presence of an orthorhombic lattice, confirming x-ray diffraction studies. Replacing the protonated free fatty acid chains by their perdeuterated counterparts demonstrates that free fatty acids and CER participate in the same orthorhombic lattice up to a level of slightly less than 1:1:0.75 cholesterol/CER/free fatty acids molar ratio but that free fatty acids also form separate domains within the lipid lamellae at equimolar ratios at room temperature. However, no evidence for this has been observed at 32°C. Extrapolating these findings to the situation in stratum corneum led us conclude that in stratum corneum, fatty acids and CER participate in the orthorhombic lattice at 32°C, the skin temperature.

INTRODUCTION

The natural function of the skin is to act as a barrier for unwanted influences from the environment. The main barrier for diffusion of substances across the skin resides in the stratum corneum, the outermost layer of the skin. The stratum corneum consists of dead flattened cells filled with water and microfibrillar keratin, which is stabilized by disulfide bonds. The corneocytes are encapsulated by a densely cross-linked layer of proteins, the cornified cell envelope (1). This envelope is covered by a chemically linked monolayer of lipids. The cornified envelope minimizes the uptake of most substances into these dead cells and therefore redirects the transport of substances along the intercellular regions (2), which are filled with a matrix of hydrophobic lipids (3). The hydrophobic lipids form lamellae, which are aligned approximately parallel to the skin surface (4). Because the main penetration pathway of substances resides in these intercellular lipid regions, the lipids are considered to play a crucial role in the skin barrier function.

The stratum corneum lipids have a very exceptional composition, as the main lipid classes are ceramides (CER), long-chain free fatty acids (FFA), and cholesterol (CHOL). The most abundant chain lengths of the FFA are 22 and 24 carbon atoms (5). In human stratum corneum, nine subclasses of CER are present (6). The CER differ from each other by the headgroup architecture and the acyl chain length. The CER consist either of a sphingosine (S), phytosphingosine (P), or a 6-hydroxysphingosine (H) base, whereas the acyl chain is either a nonhydroxy (N), an α-hydroxy (A) or an ω-hydroxy chain. The most prominent chain lengths of the nonhydroxy and α-hydroxy fatty acids are C_{24} and C_{26}. The corresponding ceramides are denoted by CER NP, CER NS, CER NH for the ceramides containing a nonhydroxy fatty acid and CER AP, CER AS and CER AH for the ceramides containing an α-hydroxy fatty acid (7). The chain length of the ω-hydroxy fatty acids varies mainly between C_{30} and C_{34}, and a linoleic acid is chemically bound to the ω-hydroxy group (referred to as EO). This results in a very exceptional molecular structure of these ceramides, which are denoted by CER EOP, CER EOS, or CER EOH. Because the penetration pathway in stratum corneum is mainly along the intercellular domains, knowledge about the lipid composition and organization of these domains is very important for understanding the skin barrier function. The lipid organization in stratum corneum has been studied by various techniques, such as electron microscopy (8,9), Fourier-transformed infrared spectroscopy (10,11), x-ray diffraction (12,13), and electron diffraction(14,15). These studies revealed that the lipids are organized in two crystalline lamellar phases with repeat distances of ~6 and 13 nm. These lamellar phases are referred to as the short periodicity phase (SPP) and the long periodicity phase (LPP), respectively. The lateral packing is mainly of orthorhombic nature, as has been identified by

Submitted August 2, 2006, and accepted for publication November 17, 2006.

Address reprint requests to Prof. J. A. Bouwstra, Leiden/Amsterdam Center for Drug Research, Gorlaeus Laboratories, Leiden University, PO Box 9502 2300 RA Leiden, The Netherlands. Tel.: 31(0)71-527-42-08; Fax: 31(0)71-527-45-65; E-mail: bouwstra@chem.leidenuniv.nl.

0006-3495/07/04/2785/11 $2.00

doi: 10.1529/biophysj.106.094292

x-ray and electron diffraction (14,16). Because the LPP has a very exceptional structure and is present in stratum corneum of all species measured until now, it has been proposed that this lamellar phase plays an important role in the skin barrier function. Very recently this has been confirmed by diffusion studies across stratum corneum substitutes prepared from stratum corneum lipids only (17), in which, in the absence of the LPP, the steady-state diffusion rate was twice that in the presence of the LPP.

Information on the relation between lipid organization and lipid composition is of great importance to unravel the mechanism controlling the skin barrier function of normal and diseased skin. In diseased skin an altered lipid composition and organization have often been identified (18–20). Because it is impossible to selectively extract lipids from stratum corneum, this relation can only be studied using mixtures prepared with either isolated or synthetic CER. When these lipid mixtures are used, the first question to be answered is: Is it possible to mimic the lipid organization in stratum corneum using mixtures prepared with CER? To answer this question, the phase behavior of mixtures prepared from either isolated human or pig CER was examined by x-ray diffraction (21–23). These studies clearly demonstrated that CER and CHOL play a crucial role in the formation of the two lamellar phases, whereas FFA increase the packing density by inducing a phase transition from a hexagonal to an orthorhombic lateral packing. However, for the formation of the LPP, it is important to equilibrate the mixtures at an elevated temperature and to incorporate acylceramides in the lipid mixtures (24–26). Very recently, a synthetic CER composition was selected mimicking the lipid phase behavior in stratum corneum very closely. However, because these CER have a well-defined chain length, both CHOL and FFA were required for the formation of the LPP (27). Although x-ray diffraction is an excellent method to study lipid phase behavior, limitations are encountered in studying the miscibility properties of the lipids in these two-dimensional lattices within the lipid lamellae. In contrast, Fourier-transformed infrared spectroscopy (FTIR) makes it possible to study the conformational ordering and miscibility of the lipids within the lattices of the lipid lamellae (28,29). In particular, the use of perdeuterated lipids allows simultaneous evaluation of the packing and miscibility properties of different classes of lipids in one lipid mixture. In addition, it permits the evaluation of the conformational order of the various lipid classes. Therefore, in the study presented here, the thermotropic behavior of mixtures prepared from CHOL, (perdeuterated) FFA, and isolated human CER was examined by FTIR to answer the central question: Are isolated CER and FFA miscible in the two-dimensional lattices in the lamellae or do these lipid classes form separate domains within the lipid lamellae? To address this question, the thermotropic behavior of the conformational ordering as well as the packing properties were examined measuring the methylene stretching, scissoring, and rocking vibrations. The methylene stretching vibrations provide information on the conformation ordering (e.g., a liquid or ordered state of the lipids), whereas the scissoring and rocking vibrations provide information on the packing properties of the lipids. Because we intended to mimic the situation in human stratum corneum as closely as possible, we decided to examine mixtures prepared with isolated human CER and FFA varying in chain length between C_{16} and C_{24}. In several experiments, however, these free fatty acids were deuterated more than 98%.

EXPERIMENTAL PROCEDURES

The perdeuterated FFA (referred to as DFFA) with chain length of $C_{16:0}$ and $C_{22:0}$ were obtained from Larodan (Malmö, Sweden). The DFFA with chain lengths of $C_{18:0}$ and $C_{20:0}$ were purchased from Cambridge Isotope laboratories (Andover, MA), and DFFA with chain length of $C_{24:0}$ was obtained from ARC laboratories (Apeldoorn, The Netherlands). Cholesterol, protonated fatty acids, and acetate buffer salts were purchased from Sigma-Aldrich Chemie GmbH (Schnelldorf, Germany). Silicagel 60 was obtained from Merck. Ceramide standards were kindly provided by Cosmoferm (Delft, The Netherlands).

Isolation of CER

Stratum corneum lipids were extracted using the method of Bligh and Dyer (30). The extracted lipids were applied on a silicagel 60 column. The various lipid classes were eluted sequentially using various solvent mixtures as published previously (20). The lipid composition of the collected fractions was established by one-dimensional high-performance thin-layer chromatography, as described earlier (31). For quantification, authentic standards were run in parallel. The quantification was performed after charring using a photodensitometer with peak integration (Bio-Rad GS 710, Bio-Rad Laboratories, Hercules, CA). The CER fractions have been mixed to achieve the composition similar to that of the human stratum corneum.

Preparation of lipid mixtures

The isolated CER were mixed with CHOL or with CHOL and FFA or CHOL and DFFA. The fatty acid mixture contained $C_{16:0}$, $C_{18:0}$, $C_{20:0}$, $C_{22:0}$, and $C_{24:0}$ in the ratio of 1.3%, 3.3%, 7%, 47%, and 41.4% (w/w). This composition has been based on the FFA composition reported by Wertz and Downing (5).

The lipid mixtures were prepared by dissolving 1.5 mg of the lipids in 200 μl of chloroform/methanol (2:1, v/v). The mixture was sprayed over an area of 1 cm^2 on an AgBr window. This was performed at a very low spraying rate (4.2 μl/min) under a gentle stream of nitrogen gas using a sample applicator (CAMAG LINOMAT IV, Muttenz, Switzerland). The sample applicator was adapted by constructing an extra axis (y direction) of spraying perpendicular on the existing axis (x direction)that allowed an application in two directions simultaneously. The AgBr window with applied lipids was heated to a temperature of 65°C and equilibrated for 10 min, after which the lipid mixture was covered with 25 μl of a deuterated acetate buffer at pH 5.0 (50 mM). We used deuterated buffer to avoid interference of the broad OH vibration peak with the CH_2 stretching vibrations. The sample was then cooled slowly at ambient temperature for 1 h. As observed with x-ray diffraction, this procedure leads to a hydration of the sample. To homogenize the sample, five freeze-thawing cycles were carried out between −20°C and room temperature.

FTIR measurements

All spectra were acquired on a Bio-Rad FTS4000 FTIR spectrometer (Cambridge, MA) equipped with a broad-band mercury cadmium telluride

detector, cooled with liquid nitrogen. The sample cell was closed by a second AgBr window. The sample was under continuous dry air purge starting 1 h before the data acquisition. The spectra were collected in transmission mode as a coaddition of 256 scans at 1 cm^{-1} resolution over 4 min. To allow detection of the phase transition, the sample temperature was increased at a heating rate of 0.25°C/min, resulting in a 1°C temperature rise during each measurement. The lipid phase behavior was examined between 20°C and 100°C. The software used was Win-IR pro 3.0 from Bio-Rad. The spectra were deconvoluted using a half-width of 5 cm^{-1} and an enhancement factor of 2.

RESULTS

Fig. 1 shows a representative infrared spectrum of the equimolar CHOL/CER/DFFA mixture. The positions of some of the major chain vibrational modes are indicated in the figure. The symmetric methylene (υsCH_2 and υsCD_2) modes provide information about the conformational order-disorder transitions, whereas the scissoring (δCH_2 and δCD_2) and rocking ($\rho_r CH_2$) modes provide information about the packing of the chains perpendicular to the chain direction. When the chains are in a crystalline orthorhombic lattice, the adjacent chains in scissoring and rocking modes interact via a short-range coupling, resulting in a broadening or splitting of the contours. The width of the splitting is an indication of the domain size of the orthorhombic lattice (32). When, however, deuterated and protonated chains are mixed in one lattice, the δCH_2 and δCD_2 modes and the $\rho_r CH_2$ and $\rho_r CD_2$ modes will not interact, and therefore, the vibrational coupling will be eradicated. In the spectrum, this will result in a disappearance of the contour splitting of the scissoring and rocking vibrations (33). Therefore, in an orthorhombic lattice, elimination of the coupling after replacing protonated lipids by deuterated ones is indicative of participation of the deuterated and protonated lipid classes in one lattice.

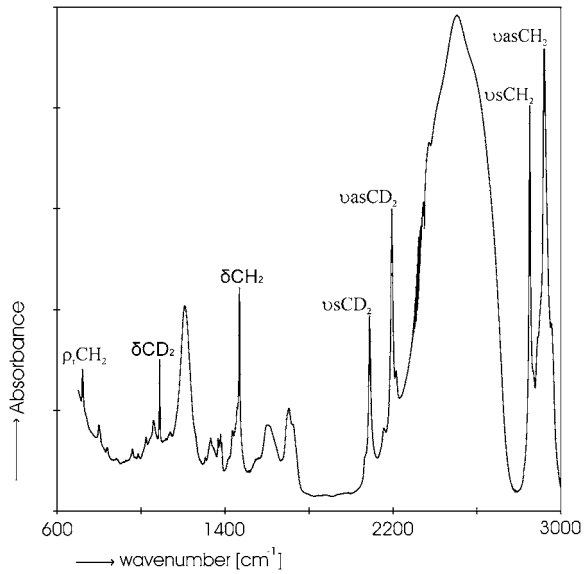

FIGURE 1 Overview of the infrared spectrum of the CHOL/CER/DFFA mixture. The asymmetric ($\upsilon asCH_2$ and $\upsilon asCD_2$) and symmetric (υsCH_2 and υsCD_2) methylene stretching modes provide information about the conformational order-disorder transitions, whereas the scissoring (δCH_2 and δCD_2) and rocking ($\rho_r CH_2$) modes provide information about the packing of the lipids perpendicular to the chain direction and are indicated in the figure.

The main classes of lipids in the stratum corneum are CHOL, CER, and FFA, and mixtures prepared from these three classes have been selected for the measurements. To determine whether CER and FFA integrate in one lattice, in some lipid mixtures protonated FFA are replaced by the deuterated counterparts. First the results of CER and DFFA mixtures without additional classes of lipids are presented. The FFA mixture behaves very similarly to the DFFA mixture.

CER mixture

Spectra are obtained from the native CER isolated from human stratum corneum. Thermotropic changes in the υsCH_2 frequency between 20°C and 100°C indicate a conformational disordering in this temperature range. As shown in Fig. 2 *A*, at 20°C the υsCH_2 frequency is at 2849.9 cm^{-1}. This frequency gradually increases until a temperature of ~60°C has been reached. Then a shift in the υsCH_2 frequency to 2853.8 cm^{-1} is encountered. This shift centered at ~73°C indicates a conformational disordering, namely a phase transition from an ordered all-*trans* solid state to a disordered fluid state. The contours of the δCH_2 and $\rho_r CH_2$ vibrations as functions of temperature are plotted in Fig. 2, *B* and *C*. At 20°C the maximum of the contour is located at ~1468 cm^{-1} with a slight splitting mainly observed for the high-frequency component, which might suggest the formation of a disordered orthorhombic lattice. In the rocking vibration contours also, a small splitting is observed with a maximum at 720 cm^{-1} and a weak shoulder at 728 cm^{-1} (see *arrow*), indicating that a very small population of the CER forms an orthorhombic lattice. This splitting dissolves at ~38°C.

DFFA mixture

Spectra are obtained from all deuterated components in the mixture. At room temperature υsCD_2 frequency at 2088.4 cm^{-1} (see Fig. 2 *A*) denotes extended, ordered all-*trans* deuterated chains. When the temperature is increased, the υsCD_2 frequencies do not change until a temperature of 68°C has been reached. At that temperature, the υsCD_2 frequency starts to shift from 2088.4 to ~2097 cm^{-1} at 86°C, indicative of an order-disorder phase transition. As far as the δCD_2 modes are concerned, a doublet is observed at 1085.4 and 1092.6 cm^{-1} (see Fig. 2, *D* and *E*). As the magnitude of the splitting (7.2 cm^{-1}) approaches its maximum value (8.4 cm^{-1}), the domain sizes are larger than 100 molecules (32) for the DFFA mixture. A similar behavior was observed for the FFA mixtures (not shown). The strong splitting of the peak is suggestive of an ordered orthorhombic lattice in the

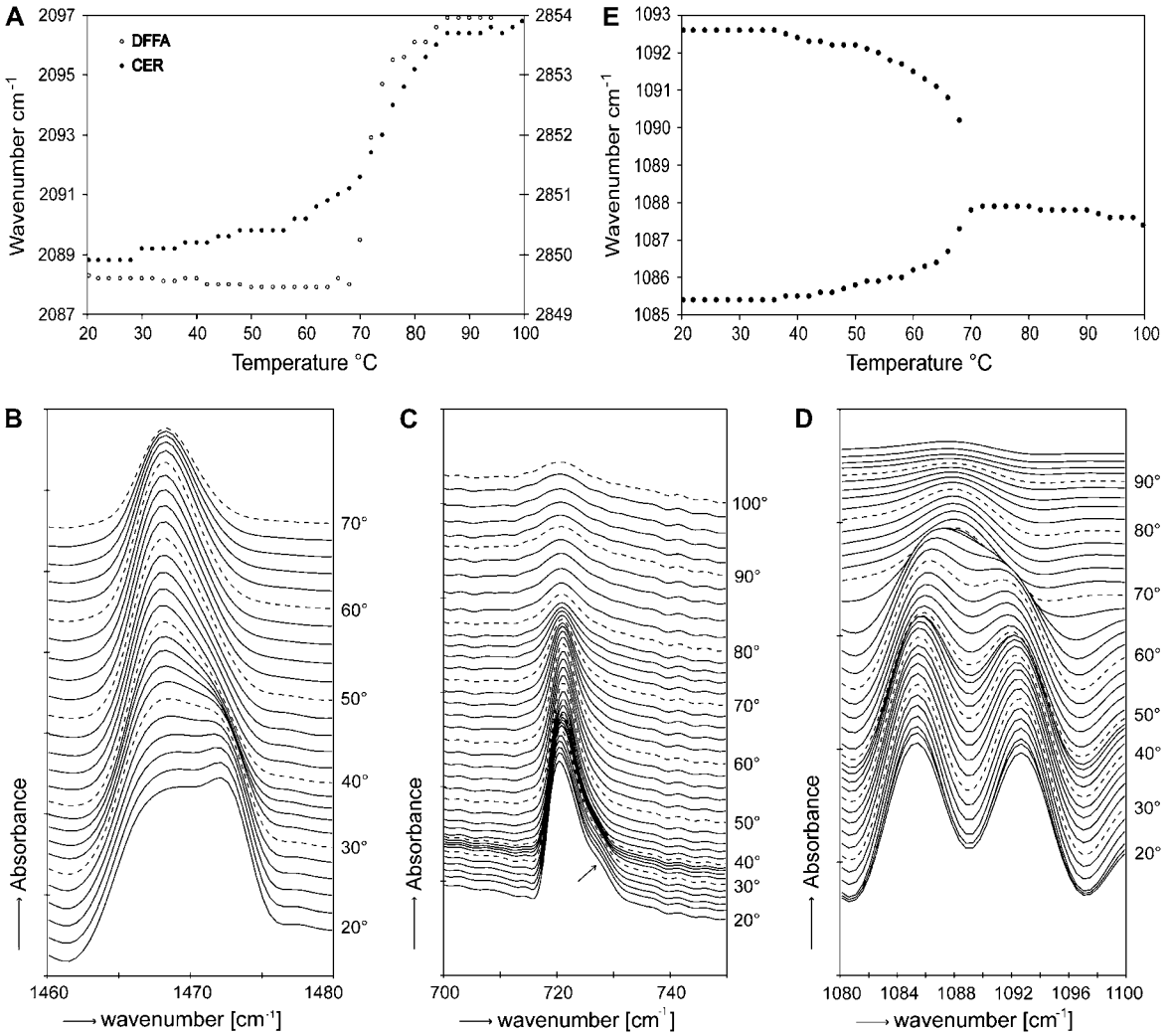

FIGURE 2 Thermotropic response and infrared spectra of CER and FFA mixtures. (*A*) The thermotropic response of the υsCH_2 modes in the CER mixture and the υsCD_2 modes in the DFFA mixture. (*B*) The original spectra of the δCH_2 modes of the CER mixture measured as a function of temperature. Note the broadening of the contour at 20°C, which disappears at ~36°C. (*C*) The original spectra of the $\rho_r CH_2$ modes of the CER mixture measured as a function of temperature. Note the weak peak at 728 cm^{-1} of the contour at 20°C, which dissolves at ~36°C. (*D*) A strong splitting of the δCD_2 contours of the DFFA mixture at 20°C. This splitting does not dissolve until a temperature of 68°C has been reached. At room temperature the maxima of the contours are located at 1085.4 and 1092.6 cm^{-1}. (*E*) The thermotropic behavior of the δCD_2 frequencies clearly demonstrating the orthorhombic-hexagonal phase change at ~68°C.

plane perpendicular to the hydrocarbon chain direction (32). The splitting collapses at ~68°C, representative of the disappearance of the orthorhombic lattice. A single peak remains at 1087.5 cm^{-1}.

CHOL/CER mixtures

The υsCH_2 stretching modes of the CHOL/CER mixture at a molar ratio of 0.4:1 have been measured between 20°C and 100°C. At 20°C the υsCH_2 vibration is located at 2849.9 cm^{-1}, representative of an ordered lattice. When the temperature increases, the peak position shifts gradually between 60°C and 80°C from 2850.6 to 2853.0 cm^{-1} (not shown). This suggests the formation of a fluid phase in a similar temperature range as observed for the DFFA and CER mixtures. The splitting of the δCH_2 mode (Fig. 3 *A*) and the broadening of the $\rho_r CH_2$ mode (Fig. 3 *B*) both disappear at ~34°C, which suggests an orthorhombic-hexagonal phase change. A further increase in CHOL level to an equimolar CHOL/CER ratio does not change the conformational ordering and vibrational frequencies at room temperature, but a gradual increase in υsCH_2 is observed between 50°C and 70°C, suggesting that the formation of a liquid phase is observed at slightly lower temperatures than in the 0.4:1 CHOL/CER mixture.

CHOL/DFFA mixtures

CHOL/DFFA = 1:1 mixtures reveal a very similar conformational ordering and vibrational frequencies as observed

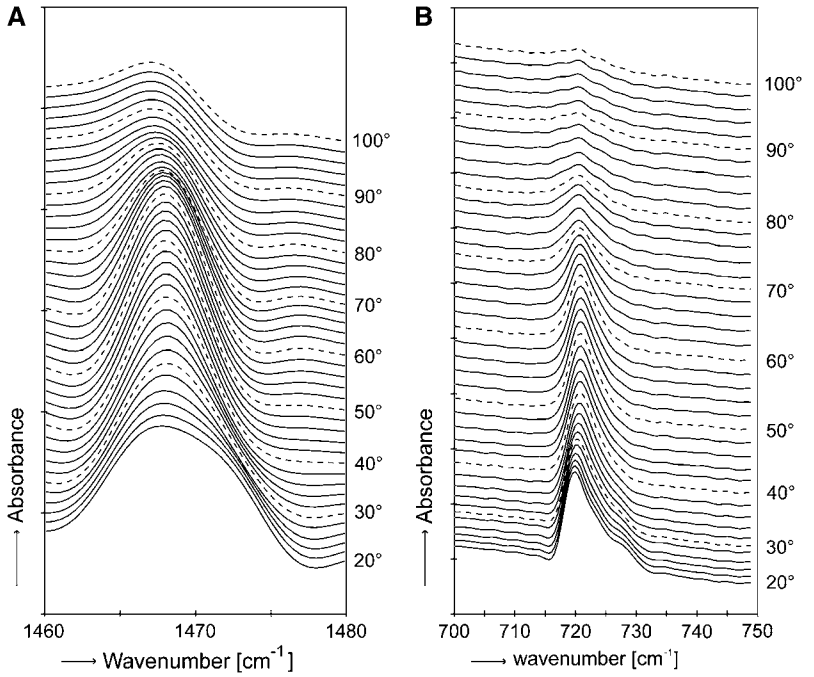

FIGURE 3 Infrared spectra of the CHOL/CER mixtures. (*A*) The original spectra of the δCH_2 modes of the 0.4:1 CHOL/CER mixture measured as a function of temperature. Note the broadening of the contour at 20°C, which disappears at ~34°C. (*B*) The original spectra of the $\rho_r CH_2$ modes of the 0.4:1 CHOL/CER mixture measured as a function of temperature.

for the DFFA mixtures. The ordered-disordered phase transition as detected by the υsCH_2 is observed at ~68°C. The splitting of the δCD_2 contours reveals an orthorhombic lattice. This splitting disappears at 68°C, similarly to that in the absence of CHOL (not shown).

CHOL/CER/FFA mixtures

Because FFA are the third major class of lipids present in stratum corneum, mixtures prepared from CER, CHOL, and FFA were also examined. First the conformational ordering and lateral packing of CHOL/CER/FFA mixtures with a molar ratio of 1:1:1, 1:1:0.75, and 1:1:0.5 are presented.

The thermotropic conformational changes as observed in the FTIR spectrum of the CHOL/CER/FFA = 1:1:1 are plotted in Fig. 4 *A*. At 20°C the υsCH_2 vibration is at 2848.9 cm^{-1}, which is slightly lower than the υsCH_2 vibration observed in the CER spectra. This decrease in υsCH_2 wavenumber compared with the CER mixtures is expected, as the CHOL/CER/FFA mixtures form mainly an orthorhombic phase (see below). On heating, a small shift of the υsCH_2 mode to a slightly higher wavenumber is observed to 2849.7 starting at ~30°C, most probably induced by an orthorhombic-hexagonal phase transition (see below). A further increase in temperature results in the formation of a disordered fluid phase in a temperature range between 60°C and 82°C as indicated by the shift in frequency to 2853.3 cm^{-1}. This shift in υsCH_2 is very similar to that noticed for the CHOL/CER and CHOL/FFA mixtures. The δCH_2 vibrations of the hydrocarbon chains reveal (Fig. 4 *B*) a splitting of the contours with vibrations at 1464 cm^{-1} and 1474 cm^{-1} at 20°C. This large splitting is indicative of an ordered orthorhombic lattice (32). Large domains are formed as the magnitude of this splitting approaches the maximum value, being 11 cm^{-1} for the δCH_2 splitting. A weak broad peak is observed at ~1468 cm^{-1}, suggesting that a small population of the lipids is not participating in the orthorhombic lattice. A gradual increase in temperature results in a collapse of the splitting and in the formation of a clear single peak at 1468 cm^{-1}. The transition from an orthorhombic to a hexagonal lattice starts at 30°C. However, at 44°C, a small population of the lipids still forms an orthorhombic phase, as can be concluded from the presence of the weak peaks at 1464 and 1472 cm^{-1}. This remaining contour splitting disappears at a temperature of ~66°C. This dual phase transition suggests that at an equimolar CHOL/CER/FFA composition phase separation occurs. This temperature-induced phase behavior has been confirmed by the changes in $\rho_r CH_2$ vibrations as a function of temperature (not shown). Whether phase separation is also observed in mixtures at a lower FFA level is shown in Fig. 4 *C*. In a CHOL/CER/FFA 1:1:0.75 mixture, the contours of the δCH_2 vibration at ~1470 cm^{-1} denote a partial splitting of the vibrations resulting in three peaks, two sharp peaks at 1464 and 1474 cm^{-1} and a central less sharp contour at 1468 cm^{-1}. This suggests that the major part of the lipids forms an orthorhombic lattice, whereas the presence of the contour at 1470 cm^{-1} denotes the coexistence of another phase, which might be either a hexagonal or a noncrystalline (e.g., liquid) phase. An increase in temperature results in a collapse of the δCH_2 splitting between 26°C and 38°C. This is in agreement with the formation of the hexagonal lateral packing observed with wide-angle x-ray diffraction (22). A further increase in temperature results in a weakening of the contours at high temperatures. The spectra of the $\rho_r CH_2$ vibrations confirm

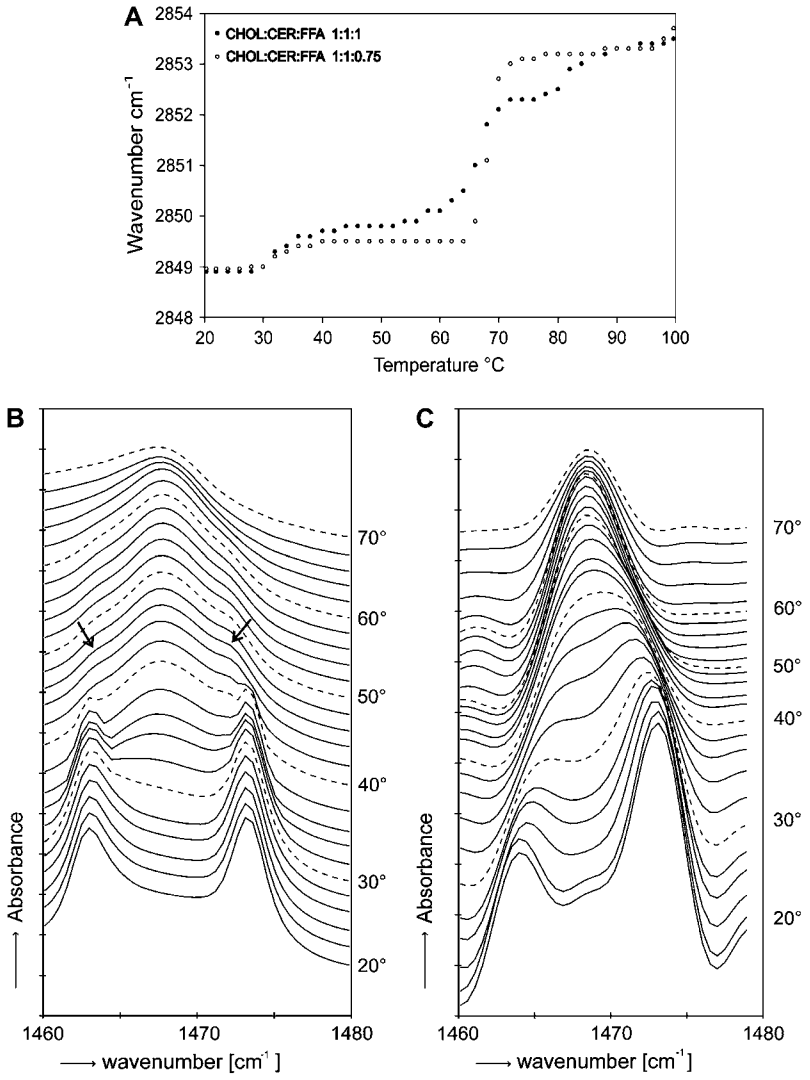

FIGURE 4 Thermotropic response and infrared spectra of the CHOL/CER/FFA mixtures. (*A*) The thermotropic response of the υsCH_2 modes in the CHOL/CER/FFA mixture. First a transition from an orthorhombic to a hexagonal phase is monitored, as shown by the small shift in υsCH_2 frequency at 30°C from 2848.9 to 2849.7 cm^{-1}. A transition from an ordered to a disordered phase is observed at 60°C to 82°C with a shift of the υsCH_2 to 2853.3 cm^{-1}. (*B*) The original spectra of the equimolar CHOL/CER/FFA mixture measured as a function of temperature. At 20°C, a strong splitting of the δCH_2 contours in the spectrum of the equimolar CHOL/CER/FFA mixture is monitored with maxima of 1464 cm^{-1} and 1474 cm^{-1} with a very weak broad peak at 1468 cm^{-1}. The splitting dissolves almost completely at a temperature of 40°C, although at higher temperatures a weak splitting is still observed (*see arrows*). This remaining splitting disappears at a temperature of 66°C. (*C*) The original spectra of the 1:1:0.75 CHOL/CER/FFA mixture measured as function of temperature. At 20°C, a strong splitting of the δCH_2 contour is monitored with a slightly stronger central peak at 1468 cm^{-1} compared with the equimolar mixture. This splitting does not dissolve until a temperature of 36°C has been reached. At room temperature, the maxima of the contours are located at 1464 and 1475 cm^{-1}. The 1468 cm^{-1} maximum suggests that a small population of lipids is also forming a hexagonal lattice.

the partial splitting at room temperature (vibrations at 719 and 729 cm^{-1}). This splitting also disappears between 26°C and 38°C (not shown).

CHOL/CER/DFFA mixtures

The short-range coupling between hydrocarbon chains in an orthorhombic lattice results in a splitting of the $\rho_r CH_2$ and δCH_2 vibrations. However, as explained above, this coupling is not present between protonated and deuterated chains in the same lattice. Therefore, if the protonated FFA are replaced by deuterated FFA, the infrared spectra provide information on the participation of CER and FFA in a single orthorhombic lattice: a reduction in the splitting of the δCD_2 vibrations in the presence of CER compared with the spectra obtained from DFFA and CHOL/DFFA mixtures indicates a partial mixing of DFFA and CER in one orthorhombic lattice. However, even if CER and DFFA form separate domains, only a weak splitting of the δCH_2 mode is expected, as a weak splitting is also observed in mixtures prepared from CER and CHOL (see Figs. 2 *B* and 3 *A*).

The δCH_2 vibrations and δCD_2 vibrations of the 1:1:1 and 1:1:0.5 CHOL/CER/DFFA mixtures are plotted in Figs. 5 and 6. First we will focus on the δCD_2 vibrations, which are presented in Fig. 5. At 20°C in the spectra of an equimolar ratio CHOL/CER/DFFA, a splitting was observed in the δCD_2 mode: the maxima of the contours are located at 1086.4 cm^{-1} and 1090.7 cm^{-1} (see Fig. 5 *A*). The splitting at this temperature, however, was less strong than that observed in the spectrum of the equimolar CHOL/DFFA and DFFA mixtures. Furthermore, the domain sizes are also much smaller, as the magnitude of splitting reduces from 7.2 to 4.3 cm^{-1} compared with that observed in the DFFA mixture. This obviously shows that a certain fraction of DFFA forms separate domains but that DFFA also participate in the same lattice as CER and CHOL. When the contours are studied at elevated temperatures, the major splitting dissolves between 26°C and 30°C into one peak located at 1089 cm^{-1}, which is

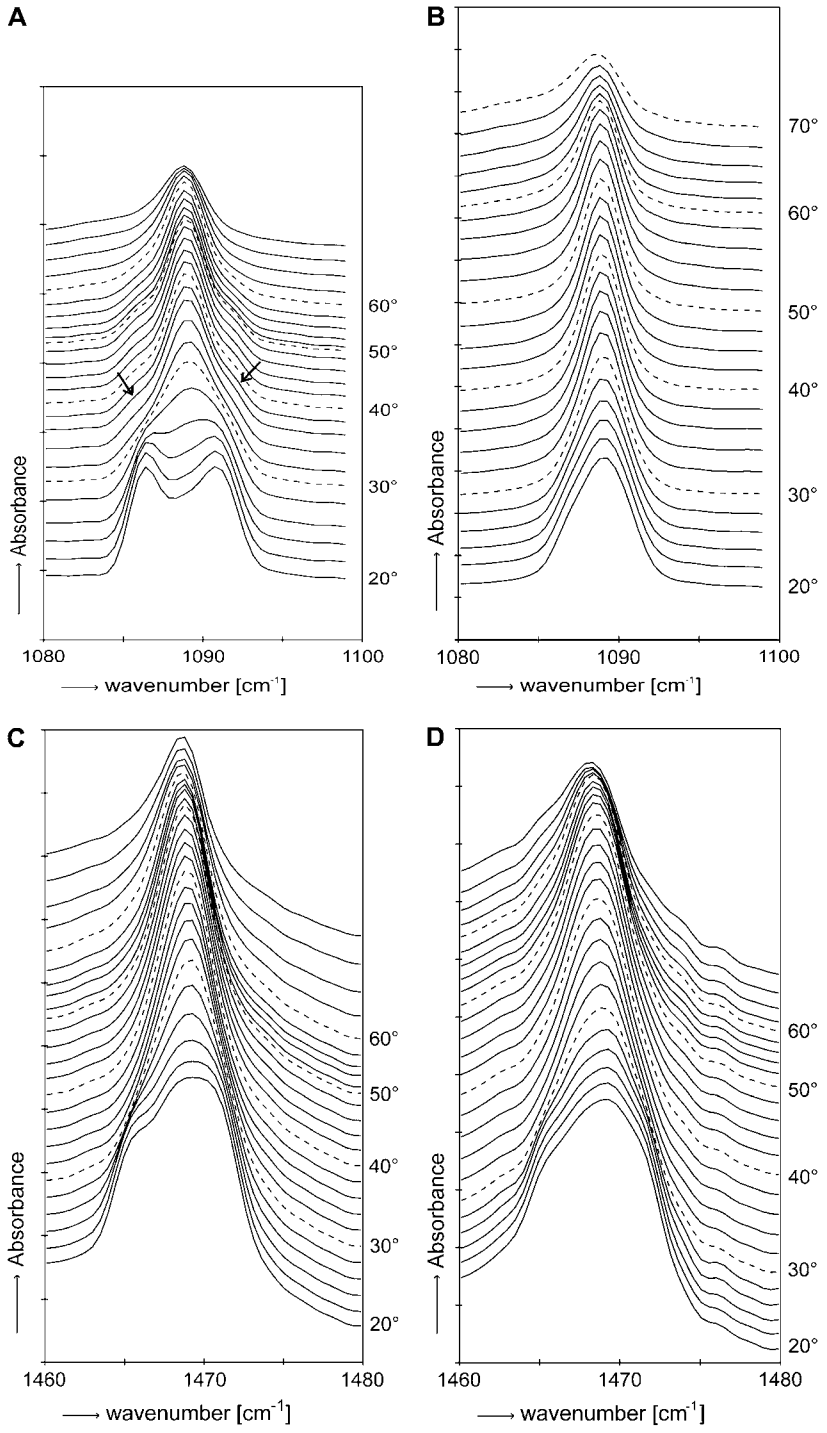

FIGURE 5 Infrared spectra of the CHOL/CER/DFFA mixtures. (*A*) The original spectra of the δCD_2 modes of the equimolar CHOL/CER/DFFA mixture as a function of temperature. At 20°C a weak splitting of the δCD_2 contours is monitored. The major part of the splitting dissolves between 26°C and 30°C, although some splitting remains (*see arrows*). At room temperature, the maxima of the contours are located at 1086.4 and 1090.7cm^{-1}, clearly demonstrating that the domain sizes of the ordered orthorhombic lattice are smaller than those of the DFFA mixture. (*B*) The original spectra of the δCD_2 modes of the 1:1:0.5 CHOL/CER/DFFA mixture as a function of temperature. Only a single δCD_2 contour is detected. (*C*) The original spectra of the δCH_2 modes of the equimolar CHOL/CER/DFFA mixture measured as a function of temperature. Note the broadening of the contour at 20°C, which gradually reduces between 24°C and 30°C. (*D*) The original spectra of the δCH_2 modes of the 1:1:0.5 CHOL/CER/DFFA mixture measured as a function of temperature. Note the broadening of the contour at 20°C, which gradually reduces between 24°C and 30°C.

at much lower temperatures than the DFFA mixture itself (see Fig. 2 *D*). However, as indicated by the arrows, a weak splitting remains at elevated temperatures. These contours weaken at ~58°C and disappear at ~62°C. This observation confirms the findings in the spectra of the equimolar CHOL/CER/FFA mixtures, which also show two weak contours of the δCH_2 mode that disappear at ~60°C. Reducing the DFFA content results in obvious changes in the δCD_2 modes. In the spectrum of the 1:1:0.75 CHOL/CER/DFFA mixture, a weak splitting in the δCD_2 contour (peaks at 1087 and 1090.5 cm^{-1}) is observed at room temperature, indicating that a decrease in the DFFA level in the mixture results in a reduced population of DFFA forming a separate domain (not shown). With a further decline in the DFFA level (Fig. 5 *B*) to a 1:1:0.5 CHOL/CER/DFFA ratio, no splitting is observed. This obviously demonstrates that at a 1:1:0.5

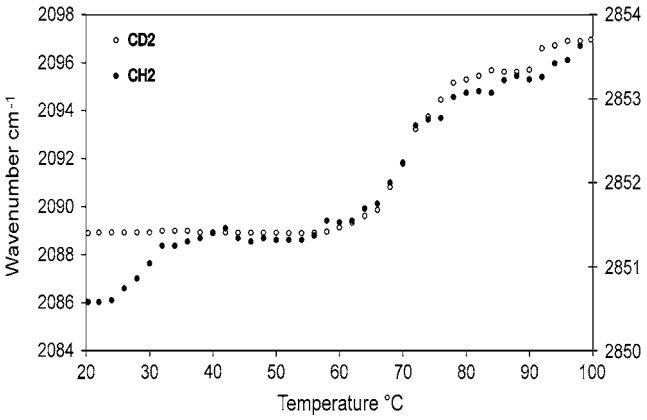

FIGURE 6 Thermotropic response of the υsCH_2 and υsCD_2 modes in the equimolar CHOL/CER/DFFA mixture. First a transition from an orthorhombic to a hexagonal phase is monitored, as shown by the small shift in υsCH_2 frequency at 30°C from 2850.5 to 2851.3 cm^{-1}. At higher temperatures, a concerted ordered-disordered transition is observed of the protonated and deuterated chains.

molar ratio DFFA is fully miscible in an ordered lattice in which an orthorhombic lattice is predominantly present. An examination of the spectra of the δCH_2 modes of the 1:1:1, 1:1:0.75, and 1:1:0.5 CHOL/CER/DFFA mixtures reveals only a very slight broadening of the δCH_2 contours positioned at 1470 cm^{-1} (see Fig. 5 *C* for the 1:1:1 composition and Fig. 5 *D* for the 1:1:0.5 composition) for all compositions. This broadening of the contour gradually reduces between 24°C and 30°C. However, the absence of a clear splitting in the δCH_2 contours does not indicate a full miscibility, as the CHOL/CER and CER mixtures do not show an obvious splitting either. As far as the stretching vibrations are concerned, the shift in peak positions of the υsCH_2 and υsCD_2 modes in the 1:1:1 and 1:1:0.5 mixtures occurs in the same temperature range (see Fig. 6), between 60°C and 78°C. This is indicative of a phase transition of the deuterated and protonated chains in the same temperature region, which suggests an associated phase change. Between 20°C and 30°C, υsCH_2 shifts to a higher wavenumber, confirming the transition from an orthorhombic to hexagonal lattice. No changes in the υsCD_2 are observed, which was unexpected, as CER and DFFA are partitioning in the same orthorhombic lattice. However, in a recent article (33) it has been noticed that the υsCD_2 are less sensitive for such a orthorhombic-hexagonal transition than the υsCH_2 vibrations.

DISCUSSION

In recent years the phase behavior of CHOL/CER and CHOL/CER/FFA prepared from isolated CER has been examined using x-ray diffraction. These studies revealed the presence of two lamellar phases, similar to those observed in human stratum corneum (21–27), and a small amount of CHOL phase separating in crystalline domains. No additional phases were observed, which led us conclude that as far as the long-range ordering is concerned, FFA and CER are distributed over the two lamellar phases, however, not necessarily with equal molar ratios in both phases. As far as the lateral packing is observed, mixtures prepared from CHOL and CER form a hexagonal lateral packing, whereas the addition of FFA induces the formation of an orthorhombic lateral packing. This has been observed not only for equimolar CHOL/CER/FFA ratios but also for mixtures with a reduced FFA level. When we compare the previous results with those presented in this article, there are some remarkable observations:

1. Mixtures prepared from isolated CER mixtures form predominantly a hexagonal lattice with a very low level of CER forming orthorhombic domains as is demonstrated by the asymmetric shape of the δCH_2 scissoring and $\rho_r CH_2$ rocking contours. After addition of CHOL to this CER mixture, the asymmetry of δCH_2 contours remain. This has been observed for the 0.4:1 and 1:1 molar ratio CHOL/CER mixtures. In similar mixtures an orthorhombic phase could not be identified using x-ray diffraction. This might be caused by the presence of only small domain sizes with an orthorhombic lattice. Small domain sizes of the orthorhombic phase can be detected by FTIR (32), whereas x-ray diffraction requires larger domains to detect the orthorhombic lattice.
2. Equimolar CHOL/CER/FFA mixtures form an orthorhombic lattice, which confirms previous results (21,22). Our study, however, shows at lower FFA levels the coexistence of the orthorhombic phase with the hexagonal phase not observed in using x-ray diffraction. In those studies only an orthorhombic phase was reported. However, because the 0.406-nm reflection of the hexagonal phase is obscured in the x-ray diffraction pattern by the strong reflection of the orthorhombic phase, it is difficult to determine whether, in addition to an orthorhombic packing, a hexagonal packing can also exist.
3. The orthorhombic-hexagonal and the hexagonal-fluid thermotropic phase transitions of the CHOL/CER/FFA mixtures occur in the same temperature range as observed with x-ray diffraction, namely between 25°C and 40°C and between 60°C and 80°C, respectively, confirming the previous results obtained with x-ray diffraction.

As far as thermotropic behavior of the FFA mixture is concerned, the ordered-disordered transition (Fig. 2 *A*) is in the same temperature region as the disappearance of the orthorhombic lattice (Fig. 2 *E*). This strongly indicates that the orthorhombic lattice transforms into a liquid phase without the formation of the intermediate hexagonal lattice. Surprisingly, rather large domains of the orthorhombic lattices are formed despite the wide chain-length distribution of this mixture.

In the literature, several excellent articles focus on the polymorphism in mixtures prepared with CER, FFA, and/or

CHOL examined by infrared spectroscopy. These studies mostly report vibrational spectra of a single CER mixed with CHOL and/or palmitic acid, stearic acid, or behenic acid. Two articles reported (34,35) the formation of large domains with limited miscibility in an equimolar hydrated mixture of bovine brain CER type III (with a variation in chain length distribution), CHOL, and palmitic acid. In an additional series of studies, CER with uniform chain length were selected. The effect of CHOL on the miscibility of stearic acid and CER NS with a uniform C_{18} acyl chain length was examined. It was shown that the two chains of pure CER NS form separate domains but that CER NS is miscible with CHOL over a wide temperature range, whereas miscibility with stearic acid was limited to elevated temperatures (36). Furthermore, CHOL affected the order-disorder transition of CER NS. In another study the effect of lipid headgroup architecture on the phase behavior was also assessed. Synthetic phytosphingosine CER appear to form more loosely packed structures than its sphingosine counterpart, and the presence of an α-hydroxy group on the acyl chain enhances the formation of hydrogen-bonding interactions in the headgroup regions (37). Interestingly, a very recent article reports that ternary hydrated mixtures prepared from stearic acid, CHOL, and CER AP with a C_{18} acyl chain form homogeneous mixtures, whereas replacement of CER AP by CER NP results in the formation of separate domains reflecting the importance of headgroup architecture in the lipid organization (38). All these studies demonstrate that the CER headgroup architecture and the presence of CHOL affect the conformation order and domain forming in these lipid mixtures. Although these studies provide interesting fundamental information on the polymorphism of mixtures and can be used to unravel the role headgroup architecture of CER plays in the lipid organization (36), the mixtures lack important aspects of the lipid composition in stratum corneum. This especially concerns the heterogeneous nature of the stratum corneum lipids, the most important characteristics being 1), the wide distribution of acyl chain lengths of the CER (5), 2), the simultaneous presence of CER based either on phytosphingosine, sphingosine, or 6-hydroxysphingosine base in one mixture (6), 3), the presence of acylceramides, and 4), the chain length distribution of the FFA varying between C_{16} and C_{26}. These characteristics of the lipid mixtures have been shown to affect the lipid phase behavior quite dramatically, namely: 1), acylceramides are crucial for the formation of the LLP that is very characteristic of the stratum corneum lipid organization (23–25), and 2), a wide distribution in fatty acid chain lengths is required to form the long and short periodicity phases without the formation of additional coexisting FFA- or CER-rich phases mimicking the lipid organization in human stratum corneum (27). However, when a single synthetic CER with a specific chain length and CHOL or a single free fatty acid are used, phase separation has been observed (39), confirming the results of most studies carried out by FTIR. Whether we use a single CER or mixtures of CER also affect the conformational disorder. In our present study we observed that the conformational ordering does not change after adding CHOL to the native CER mixtures. This is different from the observations in mixtures using a single CER. In these studies it was shown that addition of CHOL resulted in the formation of a more ordered phase (35,40,41)

Although it has been reported that human CHOL/CER/FFA mixtures form lamellar phases without the coexistence of separate FFA-rich or CER-rich phases, the question we wanted to answer in this study is: Do FFA and human CER form different domains within the lamellae, or do these lipids participate in the same orthorhombic lattice or hexagonal lattice? When CHOL/CER/FFA mixtures were used, the following observations were made:

1. The ordered-disordered phase transition occurs in the same temperature region in the FFA mixture, the CER mixture, and the CHOL/CER/FFA mixtures. Therefore, in regard to the ability to form either mixtures or separate phases, no sound conclusion can be drawn from the thermotropic phase behavior at elevated temperature.
2. Comparing the scissoring and rocking modes of the CHOL/CER/FFA and CHOL/CER/DFFA mixtures has allowed several interesting features to be observed.
   a. In equimolar CHOL/CER/FFA mixtures, a wide splitting of the rocking mode is observed at room temperature, indicating the presence of large orthorhombic domains. This splitting disappears between 30°C and 42°C, representing the orthorhombic-hexagonal phase transition.
   b. Replacing FFA by DFFA in the equimolar CHOL/CER/DFFA mixture shows that as a result of decoupling of the scissoring mode, the splitting is greatly reduced compared with mixtures with DFFA only (see Fig. 2 *D*), which is indicative of participation of CER and DFFA in the same orthorhombic lattice. However, as demonstrated by the remaining splitting of the δCD_2 contours at room temperature, a certain fraction of DFFA also forms separate orthorhombic domains. Therefore, DFFA and CER participate partially in one lattice, but to what extent? To answer this question, the DFFA level in the mixtures was reduced. At a 1:1:0.75 CHOL/CER/DFFA molar ratio, the splitting of δCD_2 contours is minimized, whereas, very interestingly, the corresponding δCH_2 contours of the 1:1:0.75 CHOL/CER/FFA mixture reveals the predominant presence of the orthorhombic lattice. A further reduction in DFFA level to a 1:1:0.5 molar ratio clearly shows a single δCD_2 contour. Therefore, the amount of FFA that participates in the lattice of the equimolar CHOL/CER mixtures exceeds 0.5 but is slightly <0.75.
   c. An important remaining question that arises is: Do FFA form separate domains within the lamellar phases,

or are these separate FFA-rich crystalline phases? This question can be answered by focusing again at the δCD_2 and δCH_2 contours. The splitting of the δCD_2 contours of the CHOL/CER/DFFA mixtures almost completely collapses at ~30°C, which is in the same temperature region as the orthorhombic-hexagonal phase transition shown by $\rho_r CH_2$ and δCH_2 contours in the CHOL/CER/FFA mixtures but clearly different from the orthorhombic-liquid transition of the DFFA and FFA mixtures. The latter starts at ~66–68°C. This shows that the thermotropic transition of FFA-rich domains is affected by the presence of CER, resulting in a concerted orthorhombic-hexagonal transition of the two domains. This strongly indicates that the fraction of FFA not participating in the orthorhombic CHOL/CER/FFA-containing lattice is mainly forming FFA-rich domains within the lamellar phases. A very weak splitting remains, however (in Figs. 3 *B* and 4 *A*), until a temperature of 60°C has been reached. It seems that a very small population of FFA still forms an orthorhombic lattice at elevated temperatures, most probably in crystalline FFA-rich domains not intercalated in the lamellar phases.

Both the previous x-ray diffraction studies (12,16,23) and present FTIR studies reveal that FFA mixtures form the densely packed orthorhombic lattice, whereas the CHOL/CER mixtures form a more open hexagonal lattice, in which the lipids have rotational freedom along their longest axis. Because the CHOL/CER/FFA mixtures also form the densely packed orthorhombic phase, it seems that FFA dictates the formation of the dominant orthorhombic lattice by incorporating CER in its structure. This is different from the CER AP/CHOL/stearic acid mixtures, in which CER AP constrains the orthorhombic organization (36).

In previous studies, it has been proposed that the repeating unit of the LPP consists of two broad crystalline layers with a central narrow layer with fluid domains. The question to be answered is: What do the observations presented in this study mean for the lipid organization in the stratum corneum? First, FFA may have an important role in establishing the skin barrier function by enhancing the formation of the very densely packed orthorhombic lattice. Second, our results also indicate that at room temperature FFA and CER integrate into one lattice up to a FFA level that is slightly lower than a FFA molar ratio of 1:1:0.75. Recently Weerheim and Ponec (42) summarized the stratum corneum lipid composition reported by a large number of groups. When these data are used to calculate the molar ratios of the main lipid classes, an approximately equimolar ratio of CHOL/CER/FFA is obtained. Therefore, the domain formation in the equimolar CHOL/CER/FFA mixture should mimic most closely the situation in human stratum corneum. Our results indicate that at room temperature the major part of the FFA fraction participates with CER in one orthorhombic lattice, whereas a minor fraction of the FFA might also form separate FFA-rich domains within the lipid lamellae. Interestingly, this splitting disappears at ~30°C (Fig. 5 *A*), which is close to the skin temperature of ~32°C, and might be an indication for the absence of separate FFA-rich domains within the lamellae at skin temperature. Third, as indicated by the scissoring modes in Fig. 3 *A*, besides the orthorhombic lattice at room temperature, a small fraction of the lipids forms either hexagonal or liquid domains. A liquid phase has also been identified with wide-angle x-ray diffraction (21) in lipid mixtures based on human CER. Current FTIR studies with deuterated linoleate of CER EOS indicate that the liquid phase is related to the presence of this linoleic acid chain (J. A. Bouwstra and G. S. Gooris, unpublished results). As it is known from studies on phopholipid membranes (43,44) that penetrants may more easily pass through sites of phase boundaries, different domains in one lipid layer would be unfavorable for establishing a good barrier function. Because the LPP consists of various lipid layers within its repeating unit, it would be of interest to study distribution of the conformational ordered and disordered domains in the various layers of the LPP. This remains to be elucidated and will certainly be a subject for future studies.

REFERENCES

1. Rice, R. H., and H. Green. 1977. The cornified envelope of terminally differentiated human epidermal keratinocytes consists of cross-linked protein. *Cell.* 11:417–422.
2. Simonetti, O., J. A. Hoogstrate, W. Bialik, J. A. Kempenaar, A. H. G. J. Schrijvers, H. E. Boddé, and M. Ponec. 1995. Visualization of diffusion pathways across the stratum corneum of native and in vitro reconstructed epidermis by confocal laser scanning microscopy. *Arch. Dermatol. Res.* 287:465–473.
3. Gray, G. M., and H. J. Yeardley. 1975. Different populations of pig epidermal cells: isolation and lipid composition. *J. Lipid Res.* 16: 441–447.
4. Madison, K. C., D. C. Swarzendruber, P. W. Wertz, and D. T. Downing. 1988. The biochemistry and function of stratum corneum. *J. Invest. Dermatol.* 90:110–116.
5. Wertz, P. W., and D. T. Downing. 1991. Epidermal lipids. *In* Physiology, Biochemistry and Molecular Biology of the Skin, 2nd ed. L. A. Goldsmith, editor. Oxford University Press, New York. 205–236.
6. Ponec, M., P. Lankhorst, A. Weerheim, and P. Wertz. 2003. New acylceramide in native and reconstructed epidermis. *J. Invest. Dermatol.* 120:581–588.
7. Motta, S. M., M. Monti, S. Sesana, R. Caputo, S. Carelli, and R. Ghidoni. 1993. Ceramide composition of psoriatic scale. *Biochim. Biophys. Acta.* 1182:147–151.
8. Breathnach, A. S., T. Goodman, C. Stolinsky, and M. J. Gross. 1973. Freeze fracture replication of cells of stratum corneum of human cells. *J. Anat.* 114:65–81.
9. Van Hal, D. A., E. Jeremiasse, H. E. Junginger, F. Spies, and J. A. Bouwstra. 1996. Structure of fully hydrated human stratum corneum: a freeze-fracture electron microscopy study. *J. Invest. Dermatol.* 106: 89–95.
10. Laugel, C., N. Yagoubi, and A. Baillet. 2005. ATR-FTIR spectroscopy: a chemometric approach for studying the lipid organisation of the stratum corneum. *Chem. Phys. Lipids.* 135:55–68.

11. Curdy, C., A. Naik, Y. N. Kalia, I. Alberti, and R. H. Guy. 2004. Non-invasive assessment of the effect of formulation excipients on stratum corneum barrier function in vivo. *Int. J. Pharm.* 271:251–256.
12. Bouwstra, J. A., G. S. Gooris, J. A. van der Spek, and W. Bras. 1991. Structural investigations on human stratum corneum by small angle x-ray scattering. *J. Invest. Dermatol.* 97:1005–1012.
13. Bouwstra, J. A., G. S. Gooris, W. Bras, and D. T. Downing. 1995. The lipid organisation of pig stratum corneum. *J. Lipid Res.* 36:685–695.
14. Pilgram, G. S. K., A. M. Engelsma-van Pelt, J. A. Bouwstra, and H. K. Koerten. 1999. Electron diffraction provides new information on human stratum corneum lipid organisation studied in relation to depth and temperature. *J. Invest. Dermatol.* 133:403–409.
15. Pilgram, G. S. K., D. C. J. Vissers, H. van der Meulen, S. Pavel, S. P. M. Lavrijsen, J. A. Bouwstra, and H. K. Koerten. 2001. Aberrant lipid organization in stratum corneum of patients with atopic dermatitis and lamellar ichtyosis. *J. Invest. Dermatol.* 117:710–717.
16 Bouwstra, J. A., G. S. Gooris, M. A. Salomons-de Vries, J.A. van der Spek, and W. Bras. 1992. Structure of human stratum corneum as function of temperature and hydration: A wide angle x-ray diffraction study. *Int. J. Pharm.* 84:205–216.
17 De Jager, M, W. Groenink, I. Bielsa, R. Guivernau, E. Andersson, N. Angelova, M. Ponec and J. A. Bouwstra. 2006. A novel in vitro percutaneous penetration model: evaluation of barrier properties with *p*-aminobenzoic acid and two of its derivatives. *Pharm Res.* 23: 951–960.
18. Lavrijsen, A. P. M., J. A. Bouwstra, G. S. Gooris, H. E. Boddé, and M. Ponec. 1995. Reduces skin barrier function parallels. Abnormal stratum corneum lipid organisation in patients with lamellar ichtyosis. *J. Invest. Dermatol.* 105:619–624.
19. Schreiner, V., G. S. Gooris, G. Lanzendörfer, S. Pfeiffer, H. Wenck, W. Diembeck, E. Proksch, and J. A. Bouwstra. 2000. Barrier characteristics of different human skin types investigated with x-ray diffraction, lipid analysis and electron microscopy imaging. *J. Invest. Dermatol.* 114:654–660.
20. Imokawa, G., A. Abe, M. Kawashima, and A. Hidano. 1991. Decreased levels of ceramides in stratum corneum of atopic dermatitis: An etiologic factor in atopic dry skin. *J. Invest. Dermatol.* 96:523–526.
21. Bouwstra, J. A., G. S. Gooris, K. Cheng, A. Weerheim, W. Bras, and M. Ponec. 1996. Phase behaviour of isolated skin lipids. *J. Lip. Res.* 37:999–1011.
22. Bouwstra, J. A., G. S. Gooris, F. E. R. Dubbelaar, and M. Ponec. 2001. Phase behaviour of lipid mixtures based on human ceramides: coexistence of crystalline and liquid phases. *J. Lipid Res.* 42:1759–1770.
23. Bouwstra, J. A., G. S. Gooris, F. E. R. Dubbelaar, A. M. Weerheim, and M. Ponec. 1998. pH and cholesterol sulfate and fatty acids affect the stratum corneum lipid organisation. *J. Invest. Dermatol. Symposium Proceedings.* 3:69–74.
24. Bouwstra, J. A., G. S. Gooris, F. E. R. Dubbelaar, A. M. Weerheim, A. P. I. Jzerman, and M. Ponec. 1998. The role of ceramide 1 in the molecular organisation of the stratum corneum lipids. *J. Lip. Res.* 39: 186–196.
25. McIntosh, T. J., M. Stewart, and D. T. Downing. 1996. X-ray diffraction analysis of isolated skin lipids: reconstitution of intercellular lipid domains. *Biochemistry.* 35:3649–3653.
26. Bouwstra, J. A., G. S. Gooris, F. E. R. Dubbelaar, and M. Ponec. 2002. Phase behaviour of lipid mixtures based on human ceramides: the role of natural and synthetic ceramide 1. *J. Invest. Dermatol.* 118: 606–616.
27. de Jager, M. W., G. S. Gooris, I. P. Dolbnya, W. Bras, M. Ponec, and J. A. Bouwstra. 2004. Novel lipid mixtures based on synthetic ceramides reproduce the unique stratum corneum lipid organization. *J. Lipid Res.* 45:923–932.
28. Snyder, R. G., H. L. Strauss, and C. Ellinger. 1982. C-H Stretching modes and the structure of *n*-alkyl chains. 1 Long, disordered chains. *J. Phys. Chem.* 86:5145–5150.
29. Snyder, R. G., G. L. Liang, H. L. Strauss, and R. Mendelsohn. 1996. IR spectroscopic study of the structure and phase behaviour of long-chain diacylphosphatidylcholines in gel-phase. *Biophys. J.* 71:3186–3198.
30. Bligh, E. G., and W. J. Dyer. 1959. A rapid method of total lipid extraction and purification. *Can. J. Biochem. Physiol.* 37:911–917.
31. Ponec, M., A. Weerheim, J. Kempenaar, A. M. Mommaas, and D. H. Nugteren. 1988. Lipid composition of cultured human keratinocytes in relation to their differentiation. *J. Lipid Res.* 29:949–961.
32. Mendelsohn, R., G. L. Liang, H. L. Strauss, and R. G. Snyder. 1995. IR spectroscopic determination of gel state miscibility in long-chain phosphatidylcholine mixtures. *Biophys. J.* 69:1987–1998.
33. Kodati, V. R., R. El-Jastimi, and M. Lafleur. 1994. Contribution of the intermolecular coupling and librotorsional mobility in the methylene stretching modes in the infrared spectra of acyl chains. *J. Phys. Chem.* 98:12191–12197.
34. Moore, D. J., M. E. Rerek, and R. Mendelsohn. 1997. Lipid domains and orthorhombic phases in model stratum corneum: evidence from fourier transform infrared spectroscopy studies. *Biochem. Biophys. Res. Commun.* 231:797–80.
35. Velkova, V., and M. Lafleur. 2002. Influence of lipid composition on the organization of skin lipid model membranes: An infrared spectroscopy investigation. *Chem. Phys. Lipids.* 117:63–74.
36. Chen, H. C., R. Mendelsohn, M. E. Rerek, and D. J. Moore. 2001. Effect of cholesterol on miscibility and phase behaviour in binary mixtures with synthetic ceramide 2 and octadecanoic acid Infrared studies. *Biochim. Biophys. Acta.* 1512:345–356.
37. Rerek, M. E., H. C. Chen, B. Markovic, D. van Wyck, P. Garidel, R. Mendelson, and D. J. Moore. 2001. Phytosphingosine and sphingosine ceramide headgroup hydrogen bonding: Structural insights through thermotropic hydrogen/deuterium exchange. *J. Phys. Chem. B.* 105:9355–9365.
38. Rerek, M. E., D. van Wyck, R. Mendelsohn, and D. J. Moore. 2005. FTIR spectroscopic studies of lipid dynamics in phytosingosine ceramide models of the stratum corneum lipid matrix. *Chem. Phys. Lipids.* 134:51–58.
39. de Jager, M. W., G. S. Gooris, I. P. Dolbnya, W. Bras, M. Ponec, and J. A. Bouwstra. 2003. The phase behaviour of skin lipid mixtures based on synthetic ceramides. *Chem. Phys. Lipids.* 124:123–134.
40. Kitson, N., J. Thewalt, M. Lafleur, and M. Bloom. 1994. A model membrane approach to the epidermal permeability barrier. *Biochemistry.* 33: 6707–6715.
41. Wegener, M., R. Neubert, W. Rettig, and S. Warterig. 1997. Structure of stratum corneum lipids characterized by FT-Raman spectroscopy and DSC. III. Mixtures of ceramides and cholesterol. *Chem. Phys. Lipids.* 88:73–82.
42. Weerheim, A., and M. Ponec. 2001. Determination of stratum corneum lipid profile by tape stripping in combination with high-performance thin-layer chromatography. *Arch. Dermatol. Res.* 292:191–199.
43. Langer, M., and S. W. Hui. 1993. Dithionitepenetration through phophilipid bilayers as a measure of defects in lipid molecular packing. *Chem. Phys. Lipids.* 65:23–30.
44. Xiang, T. X., and B. D. Anderson. 1998. Phase structures of binary lipid bilayers as revealed by permeability of small molecules. *Biochim. Biophys. Acta.* 1370:64–76.